scientific reports

OPEN

CRISPR-Cas9 screening identifies a gene signature predictive of prognosis in glioblastoma

Xing Ren[1], Xiang-rong Yao[2], Kun Chen[2], Wen-tao Xiao[3]✉ & Jun-yan He[2]✉

Glioblastoma (GBM) is the most aggressive primary brain malignancy, characterized by a poor prognosis and limited therapeutic options. Identifying essential genes and pathways involved in GBM proliferation is important for developing prognostic biomarkers and potential therapeutic targets. In this study, genome-wide CRISPR-Cas9 screening data from the dependency map (DepMap) database were analyzed to explore proliferation-related essential genes and pathways in GBM. A five-gene prognostic signature—CLSPN, HSP90B1, MED10, SAMM50, and TOMM20—was constructed using univariate, LASSO, and multivariate Cox regression analyses, and its prognostic value was evaluated in independent cohorts. Weighted gene co-expression network analysis (WGCNA) and gene set enrichment analysis (GSEA) suggested that the E2F targets pathway may be involved in GBM proliferation, consistent with the CRISPR screening results. Among the identified genes, MED10 was preliminarily implicated in regulating GBM cell proliferation and migration, as supported by functional assays. These findings propose a proliferation-related gene signature with potential prognostic relevance in GBM and indicate the E2F targets pathway as a biological process potentially associated with tumor progression. MED10 warrants further investigation as a candidate gene in the context of GBM biology and therapy.

Keywords CRISPR-cas9 screening, Glioblastoma, E2F targets pathway, Prognosis, Signature

Glioma is the most commonly diagnosed primary malignant tumor originating from astrocytes in the central nervous system, accounting for approximately 80% of all brain cancers. Among gliomas, glioblastoma (GBM) is the most aggressive and lethal subtype, comprising nearly 70% of all malignant primary brain tumors[1]. Despite advances in therapeutic strategies, the prognosis for GBM remains extremely dismal, with a median survival of only 12–15 months after diagnosis, which underscores the urgent need for improved therapeutic approaches[2]. Currently, various treatment modalities are employed to manage glioblastoma, including surgical resection, radiotherapy, chemotherapy, targeted drug delivery, gene therapy, and other adjuvant therapies[3–7]. However, GBM exhibits remarkable resistance to most existing antitumor treatments. Conventional treatment strategies fail to eradicate the entire tumor mass due to several factors, including the inability of surgery to remove all infiltrative tumor cells, the challenge of chemotherapeutic drugs crossing the blood-brain barrier, and the inherent limitations of chemotherapy and radiotherapy. Furthermore, GBM is a highly heterogeneous tumor with distinct molecular characteristics and subtypes, leading to varied clinical outcomes even under the same treatment regimen[8–10]. These challenges underscore the need for accurate patient stratification and the development of personalized and more effective therapeutic strategies.

The CRISPR/Cas9 system has revolutionized the field of genetic engineering, providing a powerful and precise tool for genome editing[11,12]. Adapted from the bacterial immune system, CRISPR/Cas9 uses a guide RNA (gRNA) to target specific DNA sequences, enabling site-specific cleavage by the Cas9 nuclease[13]. CRISPR/Cas9 is a highly specific genome editing tool that enables precise and efficient gene knockout, insertion, and modification. This system has become invaluable for studying gene function, modeling human diseases, and exploring therapeutic strategies. Its high efficiency, specificity, and versatility have made it a cornerstone technology in functional genomics. Among its numerous applications, CRISPR-Cas9 screening has emerged as a groundbreaking approach for genome-wide functional studies, providing new insights into the genetic basis of complex diseases[14–16]. This innovative screening strategy systematically knocks out genes across the genome to identify those essential for specific cellular processes, such as proliferation, survival, or drug resistance. By

[1]Clinical Laboratory Medicine Center, The First Affiliated Hospital, Hengyang Medical School, University of South China, Hengyang, China. [2]Department of Oncology, The First Affiliated Hospital, Hengyang Medical School, University of South China, Hengyang, China. [3]Department of Radiation Oncology, Affiliated Hospital of Nantong University, Nantong University, Nantong, China. ✉email: xiaowentao35@163.com; junyan_he@126.com

delivering libraries of gRNAs into cells, researchers can perform high-throughput loss-of-function screens to uncover genetic vulnerabilities or critical pathways in various biological contexts, including cancer. Notably, CRISPR-based screening has significantly advanced the discovery of therapeutic targets in challenging diseases, offering new opportunities for complex and treatment-resistant cancers like GBM.

The dependency map (DepMap) is a comprehensive and high-throughput screening project that integrates data from CRISPR/Cas9 knockout techniques to identify genes essential for tumor proliferation, metastasis, or recurrence[17]. DepMap provides two primary data formats: CERES scores and gene dependency probabilities. CERES scores quantify the effect size of knocking out a gene, normalized against non-essential and pan-essential genes, enabling the identification of genes critical for cell viability. This normalization process ensures robust comparisons across genes and cell lines, allowing researchers to detect subtle variations in gene effects, such as co-dependency relationships or the strength of killing. In contrast, gene dependency probabilities assess the likelihood that a specific gene belongs to either the non-essential or common-essential gene distribution in a cell line. This probabilistic framework is particularly valuable for binary classifications, such as distinguishing sensitive versus insensitive cell lines, and accounts for variations in screening quality across diverse experimental datasets. Importantly, genes identified as selectively essential in specific contexts are considered promising therapeutic targets, as such genes are less likely to cause toxicity in normal tissues. By combining these data formats, DepMap enables researchers to systematically explore tumor vulnerabilities, prioritize potential drug targets, and investigate prognostic biomarkers[18–22]. This integrative approach is particularly impactful for GBM research, as it offers not only new avenues for therapeutic development but also a foundation for advancing precision oncology strategies.

In this study, the DepMap database was employed to identify genes essential for GBM cell proliferation, which were subsequently analyzed to construct a robust prognostic signature for predicting overall survival (OS). The prognostic signature was established using univariate Cox regression, least absolute shrinkage and selection operator (LASSO), and multivariate Cox regression analyses. The resulting proliferation-related essential gene signature demonstrated strong predictive capability for OS in GBM patients. To further investigate the biological relevance of the identified signature, weighted correlation network analysis (WGCNA), gene ontology (GO) analysis, and gene set enrichment analysis (GSEA) were conducted. In addition, random forest analysis was applied to prioritize key genes, among which MED10 was identified as a candidate regulator of GBM progression. Preliminary functional experiments in GBM cell lines supported the potential role of MED10 in promoting cell proliferation and migration.

Several prognostic models have been proposed for GBM based on transcriptomic profiling, epigenetic features, or immune-related gene sets[23–25]. However, most of these models are constructed using differentially expressed genes or statistical associations alone, without incorporating functional genomic evidence. In contrast, our study integrates genome-scale CRISPR-Cas9 loss-of-function screening data from the DepMap project with patient-derived transcriptomic and clinical datasets to identify genes that are functionally essential for GBM cell proliferation and possess prognostic significance. This approach enhances the biological relevance of the resulting gene signature. Furthermore, we systematically investigate the underlying pathways driving the high-risk phenotype, identify potential therapeutic vulnerabilities, and perform functional validation of a key gene (MED10), thereby providing both prognostic and mechanistic insights. To the best of our knowledge, this is the first study to construct a GBM prognostic model based on CRISPR-defined essential genes and to experimentally validate one of its core components.

Methods

Datasets and processing

Gene expression profiles and clinical information for GBM patients were retrieved from The Cancer Genome Atlas (TCGA, https://portal.gdc.cancer.gov/) database ($n = 146$), while datasets CGGA325 ($n = 84$) and CGGA693 ($n = 132$) were obtained from the Chinese Glioma Genome Atlas (CGGA, https://www.cgga.org.cn/) database. Additionally, datasets including GSE74187 ($n = 59$) and GSE83300 ($n = 50$) were obtained from the Gene Expression Omnibus (GEO, https://www.ncbi.nlm.nih.gov/geo/) database. Only patients with OS longer than 30 days and complete gene expression data were included in the analysis. All datasets were preprocessed following standardized procedures, as detailed in the Methods section of the Supplementary Materials. A flowchart illustrating the study's workflow is displayed in (Fig. 1).

Identification of genes essential for proliferation of GBM cells

We used gene dependency scores to identify genes essential for GBM cell proliferation, as these scores provide a quantitative measure of gene essentiality across cell lines. CRISPR-based gene dependency information for GBM cells was obtained from the DepMap (https://depmap.org/) database. A total of 49 GBM cell lines with available CRISPRGeneDependency and CRISPRGeneEffect (CERES scores) data were included in the analysis. To ensure consistency and reliability, genes were defined as essential if their average dependency scores were more than 0.5 across all GBM cell lines. The complete list of cell lines, along with their corresponding DepMap data, is provided in (Supplementary Table S1).

GSEA

CERES scores obtained from DepMap (https://depmap.org/), which measure the effect size of knocking out a gene and are normalized against the distributions of non-essential and pan-essential genes, were utilized. To rank genes, all genes were ordered from low to high based on their average CERES scores across GBM cell lines, with lower scores indicating higher essentiality. GSEA was then performed to identify hallmark pathways enriched in GBM cell proliferation. The analysis was conducted using the R package clusterProfiler[26], and pathways with adjusted p-values < 0.05 were considered significantly enriched. Additionally, functional enrichment analyses,
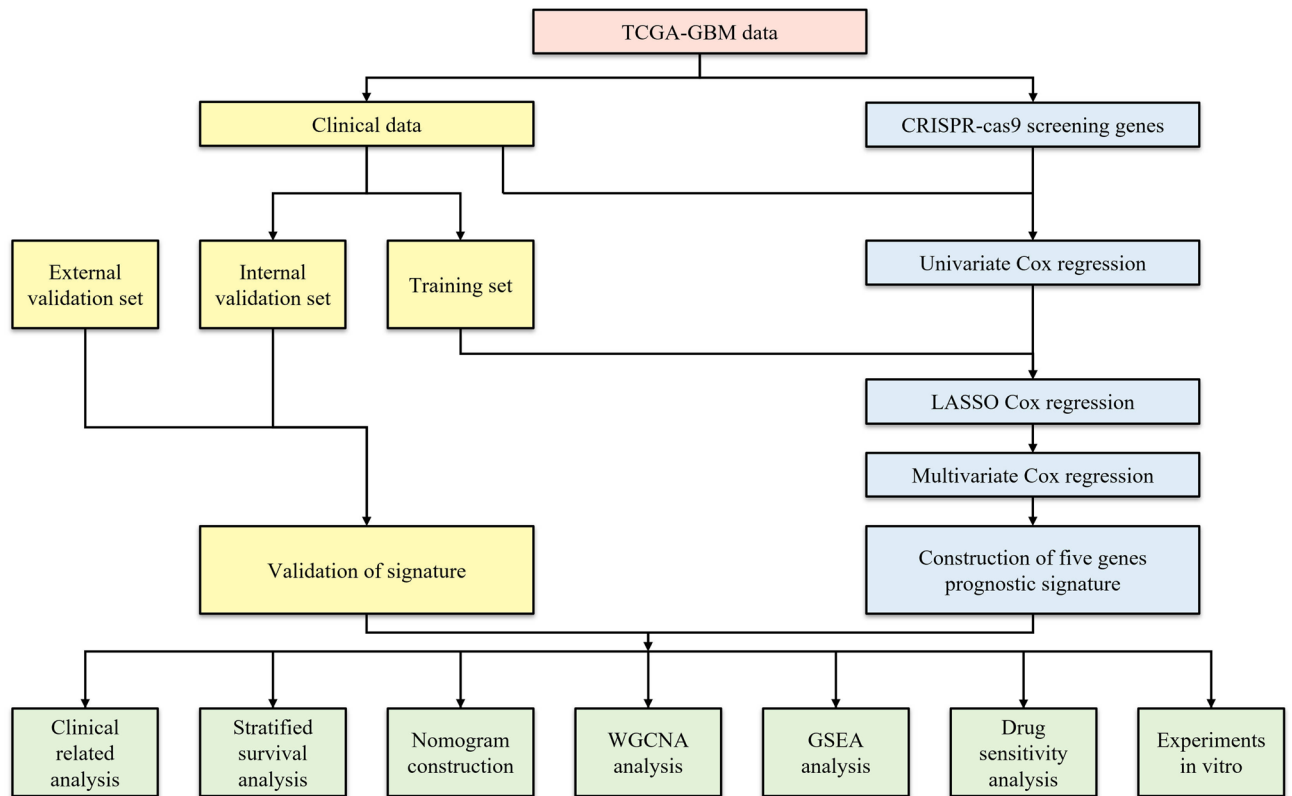
Fig. 1. The flowchart of the whole study. *TCGA* The cancer genome atlas, *GBM* glioblastoma, *LASSO* least absolute shrinkage and selection operator, *WGCNA* weighted correlation network analysis, *GSEA* gene set enrichment analysis.

including GO and KEGG[27–29] pathway enrichment, were conducted to investigate pathways associated with genes essential for GBM cell proliferation (i.e., genes with average dependency scores over 0.5). These analyses were performed using the R packages clusterProfiler and org.Hs.eg.db (https://bioconductor.org/packages/org.Hs.eg.db/).

Development and validation of the proliferation-related essential genes prognostic signature

We randomly separated the 146 cases from the TCGA-GBM dataset into training and testing groups using a 1:1 ratio. In the training group, potential OS prognostic mRNAs were initially evaluated using univariate Cox regression analysis based on genes essential for GBM cell proliferation. The glmnet R package was subsequently used to perform LASSO Cox regression analysis to select prognostic genes[30]. The selected genes were further optimized using multivariate Cox regression analysis to refine the prognostic model and ensure robustness. The risk score for each patient was calculated based on the following formula: Risk score = (exp gene1 × coef1) + (exp gene2 × coef2) + . + (exp gene n × coefn), where "exp" represents the mRNA expression value of each gene and "coef" is the coefficient of each gene obtained from multivariate Cox regression analysis. Based on the median risk score, GBM patients were stratified into low-risk and high-risk groups. Kaplan-Meier analysis was employed to evaluate survival differences between the two groups, and log-rank tests were used to assess statistical significance. Receiver operating characteristic (ROC) curve analysis was performed using 1-, 2-, and 3-year survival as endpoints to assess predictive performance through the R package pROC[31]. The area under the ROC curve (AUC), sensitivity, and specificity were used to measure predictive accuracy.

To validate the prognostic signature, two internal datasets (TCGA-test and TCGA-entire) and four external datasets (CGCA-325, CGCA-693, GSE74187, and GSE83300) were used, ensuring generalizability and robustness across independent cohorts.

Relationship between proliferation-related essential genes signature and clinicopathological features

The association between the proliferation-related essential genes signature and various clinicopathological features was analyzed using the R packages ggplot2 (https://CRAN.R-project.org/package=ggplot2), ggpubr (https://CRAN.R-project.org/package=ggpubr), and pheatmap (https://CRAN.R-project.org/package=pheatmap) to visualize trends and correlations. Stratified analyses of OS were performed using the survival (https://CRAN.R-project.org/package=survival) and survminer (https://CRAN.R-project.org/package=survminer) R packages to account for subgroup-specific effects. Additionally, univariate and multivariate Cox regression analyses were conducted using the survival R package to identify independent prognostic factors.

Nomogram construction

A prognostic nomogram integrating age, IDH status, MGMT promoter status, and the proliferation-related essential genes signature risk score was constructed using the rms (https://CRAN.R-project.org/package=rms) R package. Patients with incomplete clinical information (i.e., missing data on age, gender, IDH status, or MGMT promoter status) were excluded from this analysis, resulting in a total of 113 TCGA-GBM patients included in the nomogram construction. The nomogram's reliability was validated through calibration curves, which assessed the correlation between predicted probabilities and actual incidence rates to evaluate its predictive accuracy. Predictive performance was further quantified by calculating the concordance index (C-index) and AUC values using the riskRegression (https://CRAN.R-project.org/package=riskRegression) and timeROC[32] R packages, providing quantitative measures of the model's discriminative ability.

WGCNA

A weighted gene co-expression network was constructed using the R package WGCNA[33] to identify gene modules associated with the proliferation-related essential genes signature in the TCGA dataset. To ensure a scale-free network, a soft threshold of 12 was applied. Genes with similar expression patterns were grouped into modules, and the module most strongly correlated with the proliferation-related essential genes signature was selected for further analysis. Functional annotation and pathway enrichment analyses of this module were conducted using the R packages clusterProfiler, org.Hs.eg.db, and enrichplot (https://bioconductor.org/packages/enrichplot/) to gain insights into the biological processes and pathways underlying GBM progression.

Drug sensitivity analysis

The relationship between the proliferation-related essential genes signature and drug sensitivity was assessed using the NCI-60 cancer cell line panel, which comprises 60 tumor cell lines across a variety of cancer types and contains drug response data (Half maximal inhibitory concentration, IC50) for 792 chemotherapeutic and targeted agents. Although the panel includes a few GBM-derived cell lines, the limited number precluded a GBM-specific analysis. Therefore, a pan-cancer approach was adopted to explore potential compounds whose efficacy may be associated with the risk score derived from the GBM-specific gene signature. To apply the risk model to cell lines, we calculated the risk score for each cell line based on the expression levels of the five signature genes. Cell lines were then stratified into high-risk and low-risk groups using the median risk score as the cutoff. Tumor cell lines with more than 60% missing data were excluded to maintain the integrity and reliability of the analysis. For each drug, we evaluated the association between IC50 values and risk scores using Pearson correlation analysis. Additionally, Wilcoxon tests were performed to compare IC50 values between the two risk groups. All visualizations, including scatter plots and boxplots, were generated using the ggplot2 package in R. It is important to note that this analysis was conducted entirely at the cell line level, and no patient-derived drug sensitivity data were used in this study.

Cell culture

The glioma cell lines U118 and U87 were purchased from the Cell Bank of Chinese Academy of Sciences (Shanghai, China). U118 cells were cultured in DMEM (HyClone, USA), and U87 cells were cultured in MEM (HyClone, USA), each supplemented with 10% FBS (GIBCO, USA), 100 U/ml penicillin, and 100 μg/ml streptomycin (HyClone, USA) at 37 °C in a humidified incubator with 5% CO_2.

RNA extraction and quantitative RT-PCR analysis

Total RNA was isolated using TRIzol reagent (Ambion, Austin, TX, USA) according to the manufacturer's instructions. The concentration and purity of RNA were determined using a NanoDrop One spectrophotometer (Thermo Scientific, USA). cDNA was synthesized from 1 μg of total RNA using the PrimeScript RT reagent kit (TaKaRa, Beijing, China). Target gene expression was quantified using the SYBR Green PCR Kit (TIANGEN, Beijing, China), with GAPDH serving as the internal control. Relative mRNA expression levels were calculated using the 2 − ΔΔCt method. The qPCR primer sequences are as follows:

MED10
5′- ATCGTCAGTGACTTCCAGCC – 3′ (forward).
    5′- CCTCTCCAGGCACTCTTTGG – 3′(reverse).

GAPDH
5′- TGGTATGAGAGCTGGGGAAT – 3′ (forward).
    5′- GGACTGTGGTCTGCAAAAGG – 3′(reverse).

MED10 knockdown

To knock down the expression of MED10, two specific small interfering RNAs (siRNAs) targeting the MED10 mRNA sequence were identified and synthesized by Shanghai GenePharma Company. Transient transfection of the siRNAs was conducted using Lipofectamine 3000 (Invitrogen) according to the manufacturer's instructions. A scrambled siRNA (si-NC) was used as the negative control to ensure specificity. The sequences of the MED10-siRNAs used are as follows:

si-NC
(sense: 5′- UUCUCCGAACGUGUCACGUTT – 3′; antisense: 5′- ACGUGACACGUUCGGAGAATT – 3′)

4

MED10-siRNA-1
(sense: 5′- CUGGCUUACAGGAUAUUGATT – 3′; antisense: 5′- UCAAUAUCCUGUAAGCCAGTT – 3′)

MED10-siRNA-2
(sense: 5′ - GCAAGAUCGACACCAUGAATT – 3′; antisense: 5′- UUCAUGGUGUCGAUCUUGCTT – 3′)

Cell proliferation assay

The proliferative ability of glioblastoma cells was assessed using the Cell Counting Kit-8 (CCK-8) assay (Dojindo, Kumamoto, Japan) and a colony formation assay. In the CCK-8 assay, cells were seeded in 96-well plates (2000 cells/well), cultured for 24 h, then transfected with siRNAs. The optical density was measured at 450 nm at 24, 48, and 72 h post-transfection using a microplate reader (Sunrise, Tecan; Switzerland). To ensure reproducibility, each experimental group included three biological replicates. For the colony formation assay, 500 transfected cells were plated in 6-well plates and cultured for 12 days, with the medium being changed every four days. All cell colonies were fixed in methanol for one hour and stained with Giemsa for two hours at room temperature. Colonies were counted manually and images were obtained using an image scanner. Both experiments were conducted in triplicate.

Migration assays

Migration assays were performed to assess the migratory ability of GBM cells. U118 and U87 cells were cultured until they reached approximately 90% confluence. The monolayer was washed with PBS to remove dislodged cellular debris, and a 10 μL pipette tip was used to create a scratch across the cell layer. Cells were then cultured in serum-free medium for 24 h. Images of the scratches were captured under a microscope (Olympus, Japan) before and after the incubation period to evaluate cell migration. The migration rate was calculated as the percentage of the scratch area covered by cells after 24 h.

Statistical analysis

All data analyses were conducted using R (version 4.2.2), with a significance threshold set at $p < 0.05$. Experimental data were analyzed using GraphPad Prism (version 9.5). For robustness, a minimum of three independent experimental datasets were analyzed using a two-tailed t-test to assess differences between groups. Details of statistical tests and assumption checks are provided in the Supplementary Methods. Statistical significance was denoted as follows: *$P < 0.05$, **$P < 0.01$, ***$P < 0.001$, ****$P < 0.0001$.

Results

Proliferation-related essential genes of GBM cell identified by CRISPR knockout screen database

From the DepMap database, genome-wide CRISPR-based loss-of-function assays were utilized to identify candidate proliferation-related essential genes implicated in GBM. Firstly, we used CERES scores to explore the main hallmark pathways affecting GBM cell line proliferation through GSEA analysis. As shown in Fig. 2a, the hallmark pathways that promote the proliferation of GBM cell lines include MYC targets, oxidative phosphorylation, E2F targets, G2M checkpoint, DNA repair, and mitotic spindle, among others. Based on the normalized enrichment score (NES), the top five pathways with the highest significance were displayed in (Fig. 2b).

Then, to identify which genes are important for GBM cell growth, we looked at gene dependency scores for all GBM cell lines in the DepMap database. Genes with an average dependency score over than 0.5 in all GBM cell lines were considered essential for cell growth and were labeled as proliferation-related essential genes for GBM. Upon analysis, we found that there are 1618 proliferation-related essential genes in GBM cells (Table S2). Furthermore, the GO enrichment analysis revealed that the proliferation-related essential genes were mainly enriched in ribonucleoprotein complex biogenesis, spliceosomal complex, and catalytic activity acting on RNA (Fig. 2c). In addition, KEGG enrichment analysis identified the spliceosome pathway as the most significantly enriched pathway (Fig. 2d).

Construction and validation of the proliferation-related essential genes prognostic signature

Initially, all cases in the TCGA-GBM dataset were divided randomly into a training cohort ($n = 73$) and a test cohort ($n = 73$). Subsequently, using the univariate Cox and LASSO Cox regression analysis, and the top-performing model comprised of eight genes, namely ANKLE2, CLSPN, CUL1, HSP90B1, MED10, SAMM50, TOMM20, and WAC (Fig. 3a,b). These genes were then subjected to stepwise multivariate Cox regression analysis to determine the optimal combination of prognostic markers. As shown in Fig. 3c, five genes (MED10, CLSPN, HSP90B1, SAMM50, and TOMM20) were retained in the final model. Among them, MED10 exhibited the highest hazard ratio (HR = 2.76, 95% CI: 1.16–6.7, $p = 0.022$), indicating a strong independent association with poor survival. CLSPN (HR = 1.72, $p = 0.005$) and HSP90B1 (HR = 1.96, $p = 0.030$) also remained statistically significant after adjustment, suggesting their roles as independent risk factors. In contrast, SAMM50 and TOMM20 had hazard ratios less than 1, indicating potential protective effects, although their p-values (0.098 and 0.051, respectively) did not reach statistical significance. These results support the inclusion of both risk- and protection-associated genes in the final prognostic signature.

The risk score model was established as follows: Risk score = 0.5440 × CLSPN + 0.6712 × HSP90B1 + 1.0263 × MED10 + (-0.6918) × SAMM50 + (-0.8709) × TOMM20 (Fig. 3d). All patients were classified into high- and low-risk score groups using the median risk score. Figure 3e illustrates the distribution of risk scores, survival times, and patient stratification into the two risk groups, while Fig. 3f shows the expression levels of the five genes across the groups. As shown in Fig. 3g, our survival analysis revealed a significant difference between the
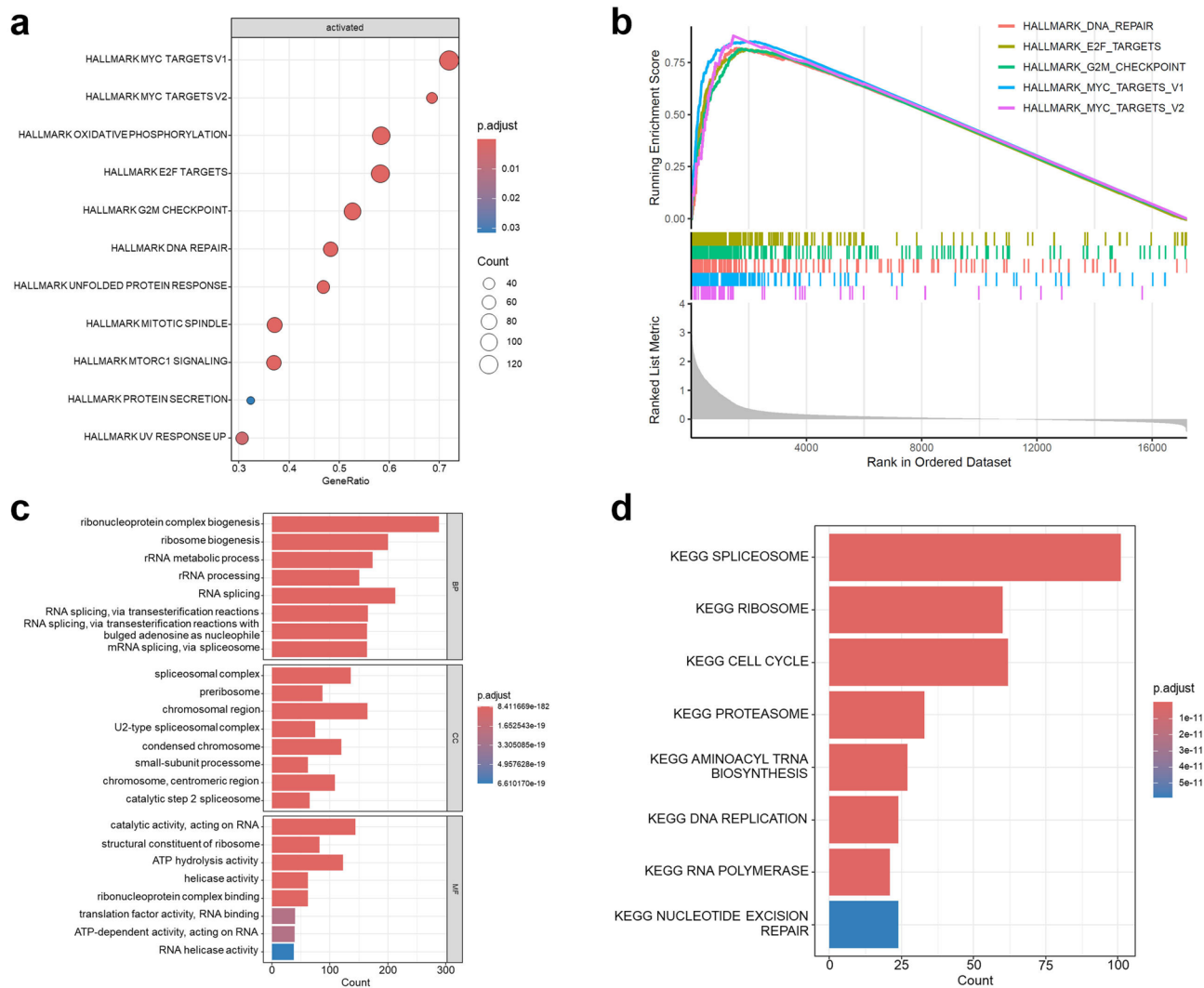
Fig. 2. Identification of proliferation-related essential genes and pathways in glioblastoma using CRISPR-based loss-of-function screening. (**a**) Hallmark pathway enrichment analysis of glioblastoma proliferation-related essential genes based on CERES scores. (**b**) Top 5 hallmark pathways ranked by NES. (**c**) GO enrichment analysis of the identified proliferation-related essential genes. (**d**) KEGG pathway enrichment analysis of proliferation-related essential genes. *NES* normalized enrichment scores, *GO* gene ontology, *KEGG* kyoto encyclopedia of genes and genomes, *BP* biological process, *CC* cell component, *MF* molecular function.

two risk groups, with the low-risk group exhibiting significantly more favorable outcomes compared to the high-risk group. The ROC plots were utilized to assess the dependability of the model, and it was indicated that the area under the AUC values for 1-, 2-, and 3-year OS rates were 0.708, 0.969, and 0.951, respectively, indicating the strong predictive potential of the signature (Fig. 3h). Lastly, the chromosomal positions of these five genes are shown in (Fig. 3i).

To assess the robustness of the proliferation-related essential genes signature, we conducted survival and ROC analyses in two internal cohorts (TCGA-test and TCGA-entire) and four external validation cohorts (CGCA-325, CGCA-693, GSE74187, and GSE83300). The distribution of the gene expression, risk scores, and survival statuses of GBM patients were shown in (Fig. 4a). Kaplan-Meier survival analysis showed that the low-risk group had better survival outcomes compared to the high-risk group, as illustrated in both the internal and external cohorts (Fig. 4b), which were consistent with those from the training cohort. Additionally, ROC analysis indicated that the AUC values for the internal and external cohorts demonstrated high predictive reliability, as shown in (Fig. 4c), further emphasizing the robustness of the predictive signature.

Relationship between proliferation-related essential genes signature and clinicopathological features

To assess the clinical potential of our signature, a comprehensive clinical association analysis was conducted. The heatmap and boxplot (Fig. 5a,b) demonstrated that the proliferation-related essential genes signature was significantly associated with key clinicopathological features, including age and IDH status. Our results indicated
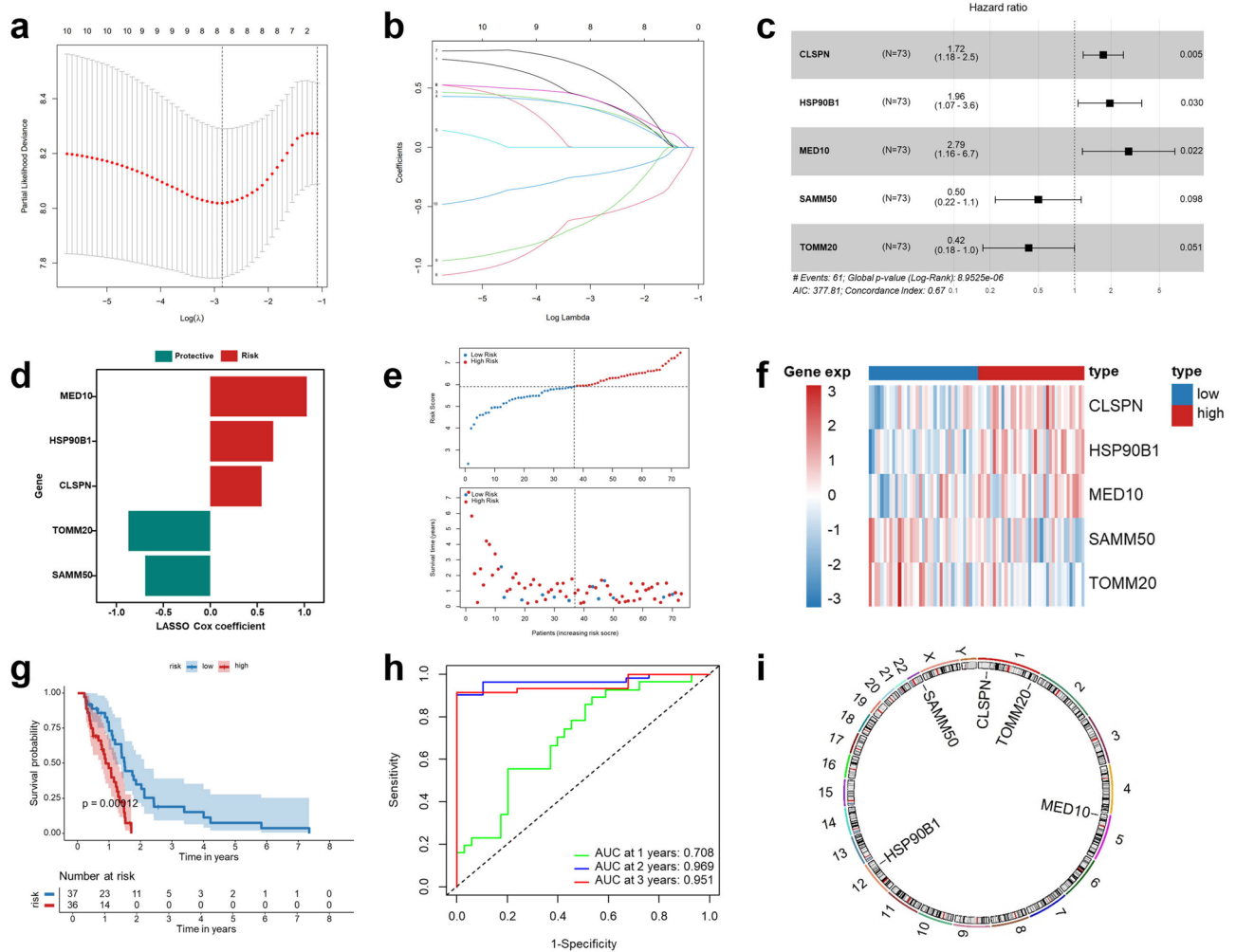
Fig. 3. Construction of the proliferation-related essential genes prognostic signature for glioblastoma. (**a,b**) LASSO regression analysis of prognostic proliferation-related essential genes. (**c**) Five prognostic proliferation-related essential genes (CLSPN, HSP90B1, MED10, SAMM50, TOMM20) were identified by multivariate Cox regression analysis. (**d**) Risk coefficients of the five prognostic genes. (**e**) Distribution of risk scores (top) and survival status (bottom) of glioblastoma patients. (**f**) Heatmap of the expression levels of the five genes across high- and low-risk groups. (**g**) Kaplan-Meier survival analysis showing significantly worse overall survival in the high-risk group compared to the low-risk group. (**h**) ROC curves evaluating the predictive performance of the prognostic signature for 1-, 2-, and 3-year overall survival. (**i**) Chromosomal locations of the five genes in the prognostic signature. *LASSO* least absolute shrinkage and selection operator, *ROC* receiver operating characteristic, *AUC* area under curve.

that patients with older age (age > 60 years) and IDH wild type (WT) exhibited significantly higher risk scores compared to younger age (age ≤ 60 years) and IDH mutant, respectively. The hierarchical analysis revealed that patients with high-risk scores tended to have poorer OS across various subgroups stratified by age, gender, IDH status, and MGMT promoter status (Fig. 5c–j). Notably, the signature retained its prognostic value across these diverse clinical subcategories, further supporting its robustness. In addition, univariate and multivariate Cox regression analyses were performed to evaluate whether our signature was an independent prognostic factor for GBM patients. The results showed that the risk score and MGMT promoter status were independent prognostic factors, indicating that the risk score could independently predict the prognosis of GBM patients, regardless of other clinical variables (Fig. 6a,b). Specifically, in the multivariate analysis, the risk score showed a hazard ratio of 1.612 (95% CI: 1.175–2.212, $p = 0.003$), while MGMT promoter methylation was also significantly associated with better survival (HR = 1.688, 95% CI: 1.074–2.655, $p = 0.023$). These results further support the independent prognostic value of the signature.

Nomogram construction

To further enhance the clinical utility of our findings, a nomogram model was formulated based on significant prognostic factors, including age, IDH status, MGMT promoter status, and risk score, as illustrated in (Fig. 6c). The nomogram provides an intuitive and practical statistical tool for predicting GBM patients' survival, enabling
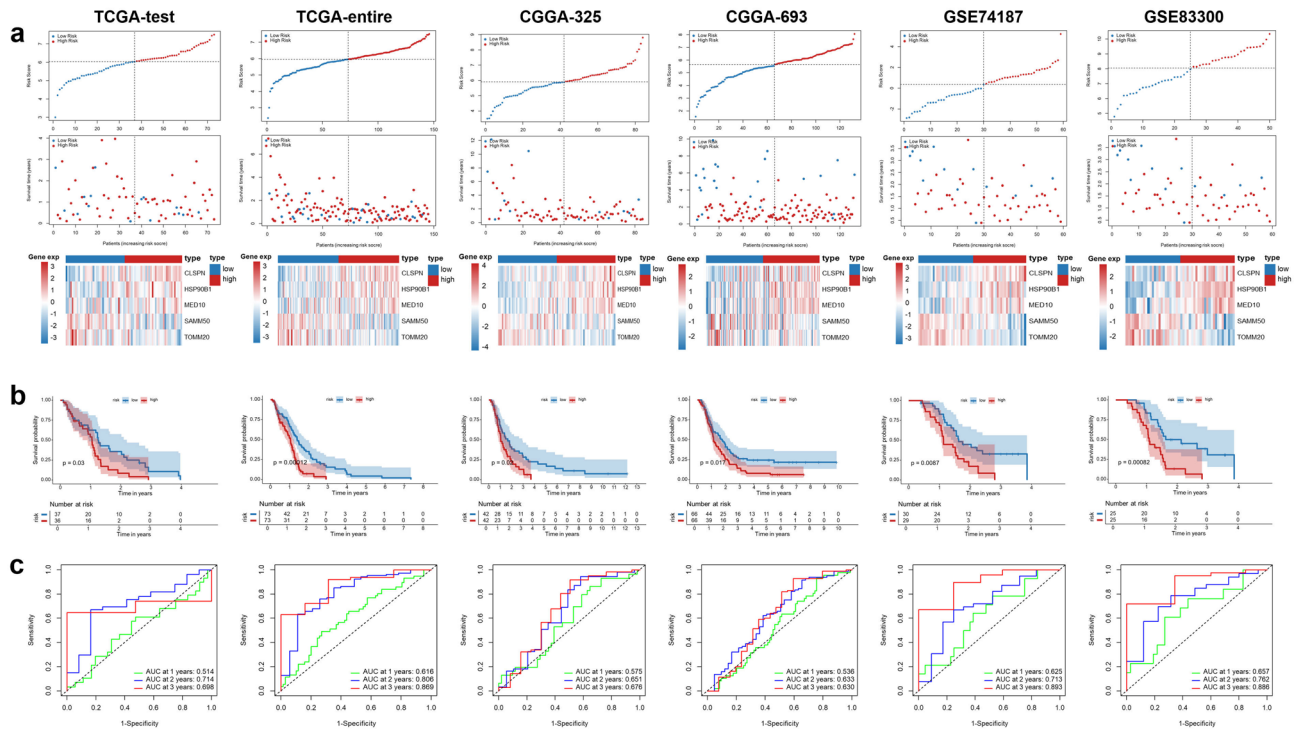
Fig. 4. Validation of the proliferation-related essential genes prognostic signature in internal and external cohorts. (**a**) Distribution of risk scores (top), survival status (middle), and expression levels of the five signature genes (bottom) in glioblastoma patients across two internal cohorts (TCGA-test and TCGA-entire) and four external cohorts (CGGA-325, CGGA-693, GSE74187, GSE83300). (**b**) Kaplan-Meier survival curves for internal and external cohorts, showing significantly poorer overall survival in the high-risk group compared to the low-risk group. (**c**) ROC curves demonstrating the predictive performance of the prognostic signature in each cohort. *TCGA* the cancer genome atlas, *CGGA* Chinese glioma genome atlas, *ROC* receiver operating characteristic, *AUC* area under curve.

the risk model to be applied in clinical practice. The outcomes revealed that our nomogram exhibited impressive capability in predicting the 1-, 2-, and 3-year OS for GBM patients, as depicted in (Fig. 6d). The C-index of the nomogram was notably higher compared to the predictive capability of using single indices alone (Fig. 6e), highlighting the superiority of the integrated model. Furthermore, Kaplan-Meier survival analysis revealed that patients with high nomogram scores exhibited significantly poorer OS, as shown in (Fig. 6f). The nomogram's ROC AUC values for predicting 1-, 2-, and 3-year OS were 0.659, 0.863, and 0.909, respectively (Fig. 6g). These results underscore the robust performance and clinical relevance of the signature-based nomogram in reliably predicting the prognosis of GBM patients.

WGCNA and GSEA

We constructed a WGCNA network to explore the regulatory relationships associated with the proliferation-related essential genes signature in GBM. A soft threshold β of 12 was applied, leading to the identification of 16 distinct gene modules using the topological overlap matrix (Fig. 7a,b). These modules were labeled as follows: pink (801), green (1057), greenyellow (356), cyan (198), magenta (740), black (837), tan (275), brown (1768), yellow (1339), salmon (220), blue (2131), purple (386), turquoise (2677), midnightblue (182), red (929), and grey (3588) (Fig. 7b). Among these modules, the magenta and turquoise modules were of particular interest due to their strongest correlation with the risk score. Subsequent analysis demonstrated that the magenta module exhibited the strongest positive correlation with the risk score (correlation coefficient = 0.54, $p = 3.1e-57$) (Fig. 7c), while the turquoise module exhibited the strongest negative correlation with the risk score (correlation coefficient = -0.35, $p = 5.4e-78$) (Fig. 7d). GO enrichment analysis revealed that genes within these modules were predominantly associated with ribonucleoprotein complex biogenesis, the ribosome, and catalytic activity acting on RNA (Fig. 7e). In addition, KEGG enrichment analysis identified Huntington's disease, oxidative phosphorylation, ribosome, and cell cycle pathways as the most significantly enriched pathways (Fig. 7f). Furthermore, Hallmark pathway enrichment analysis highlighted that these genes were primarily involved in cell proliferation processes, including E2F targets, MYC targets V1, G2M checkpoint, and MYC targets V2 (Fig. 7g).

To further elucidate the potential biological mechanisms underlying the significant survival differences between high-risk and low-risk groups in this proliferation-related essential genes signature, GSEA analysis was performed. Hallmark pathway enrichment analysis identified several signature-associated signaling pathways, including E2F targets, G2M checkpoint, oxidative phosphorylation, TNF-α signaling via NF-κB, epithelial-mesenchymal transition (EMT), and mitotic spindle, among others (Fig. 8a). Interestingly, many of
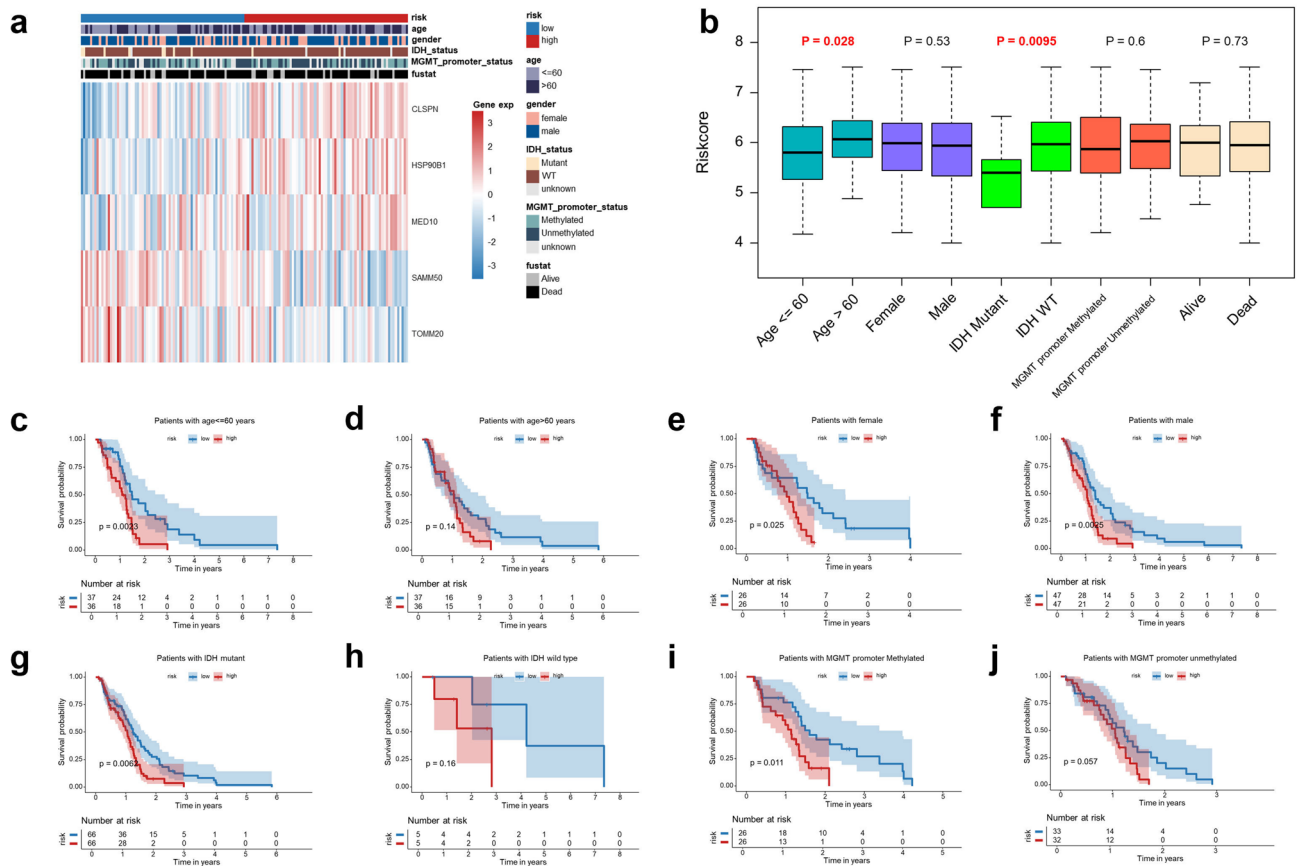
Fig. 5. Association between the proliferation-related essential genes signature and clinicopathological features in glioblastoma patients. (**a**) Heatmap displaying the relationship between the risk score, clinicopathological features (age, gender, IDH status, MGMT promoter status, and survival status), and the expression of the five signature genes. (**b**) Boxplots illustrating the distribution of risk scores across clinicopathological subgroups. (**c–j**) Kaplan-Meier survival curves for glioblastoma patients stratified by age, gender, IDH status, and MGMT promoter status.

these pathways overlapped with those identified in the magenta and turquoise modules, particularly the cell proliferation processes. Notably, E2F targets, G2M checkpoint, and mitotic spindle were significantly activated in the high-risk group (Fig. 8b–d). Other oncogenic pathways, such as TNF-α signaling via NF-κB, EMT, and angiogenesis, were also significantly activated in the high-risk group (Fig. 8e–g).

GSEA of CERES scores from CRISPR-Cas9 screening identified the E2F targets pathway as one of the most significantly enriched pathways driving GBM cell line proliferation. Moreover, WGCNA and GSEA of the proliferation-related essential genes signature in TCGA-GBM data further identified the E2F targets pathway as the most significantly enriched. These consistent findings underscore the pivotal role of the E2F targets pathway in GBM proliferation. Collectively, findings from CRISPR-Cas9 screening and TCGA-GBM analyses consistently pinpointed the E2F targets pathway as a key driver of GBM proliferation, showing significant enrichment in proliferation-related essential genes and a strong association with high-risk glioblastoma.

Correlation between proliferation-related essential genes signature and drug sensitivity

To identify potential therapeutic drugs for patients in the high-risk group, we conducted an analysis of the relationship between the proliferation-related essential genes signature and drug sensitivity. Our analysis revealed a significant negative correlation between the proliferation-related essential genes signature and sensitivity to several drugs, including Denileukin Diftitox (Ontak), Vorinostat, Entinostat, Quisinostat, AFP464, Tipifarnib, JZL-195, Ixabepilone, and RO-5,126,766 (Fig. 9a). The IC50 values for patients in the high-risk group were significantly lower, indicating that these patients may be more sensitive to these drugs (Fig. 9b). This suggests that these drugs may serve as promising therapeutic options for improving outcomes in high-risk GBM patients.

Identification of MED10 as the most important gene in proliferation-related essential genes signature

Subsequently, we performed random forest analysis to identify the most important gene within the proliferation-related essential genes signature for further investigation. Our analysis revealed that MED10 was the most significant gene among the five proliferation-related essential genes (Fig. 10a–c). Kaplan-Meier survival analysis
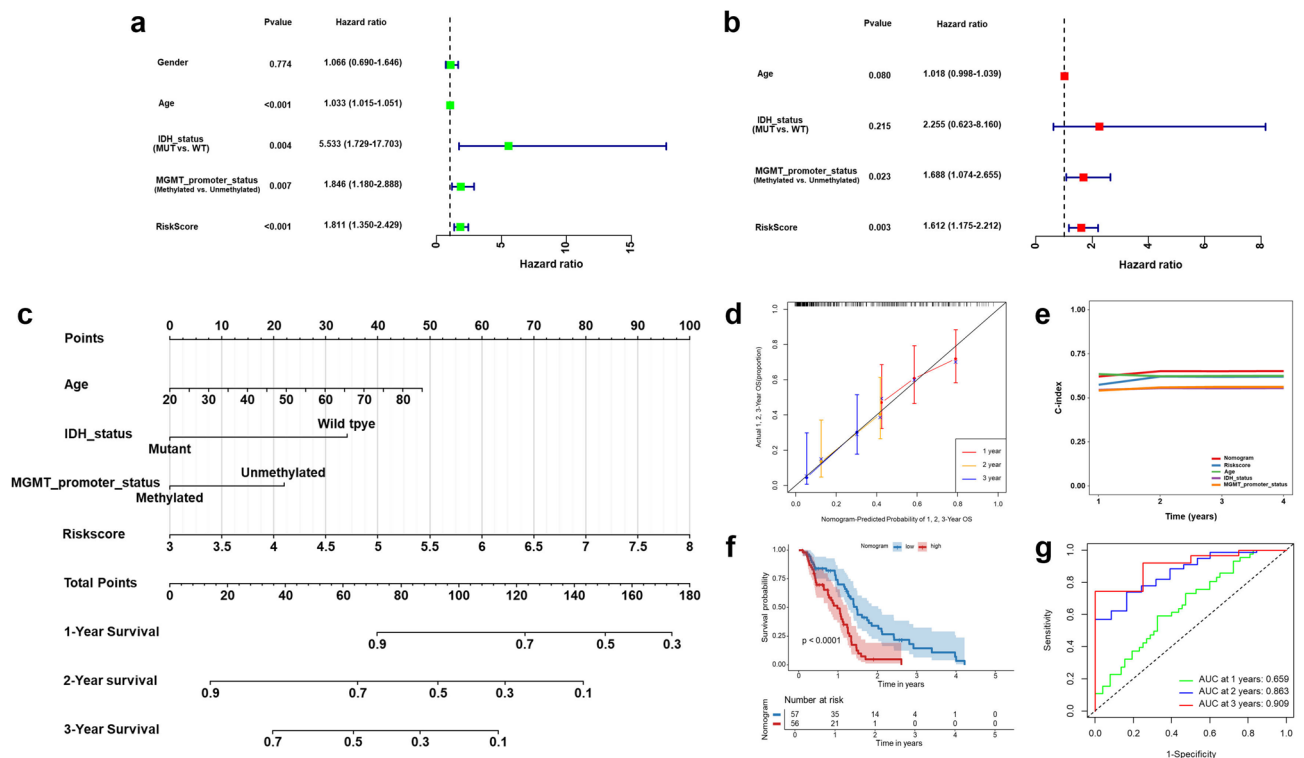
Fig. 6. Construction and validation of a nomogram for predicting glioblastoma patients' overall survival. (**a,b**) Univariate Cox regression and multivariate Cox regression analysis of clinicopathological factors and risk score. (**c**) Nomogram integrating significant prognostic factors (age, IDH status, MGMT promoter status, and risk score) for predicting 1-, 2-, and 3-year OS in glioblastoma patients. (**d**) Calibration curves demonstrating the accuracy of the nomogram in predicting survival probabilities at 1, 2, and 3 years. (**e**) Comparison of C-index values for the nomogram and individual predictors. (**f**) Kaplan-Meier survival analysis based on nomogram scores. (**g**) ROC curves assessing the predictive capability of the nomogram for 1-, 2-, and 3-year overall survival. *OS* overall survival, *ROC* receiver operating characteristic, *AUC* area under curve.

demonstrated that patients with high MED10 expression had significantly worse OS compared to those with low MED10 expression in GBM patients (Fig. 10d–g). Moreover, the CRISPR gene effect of MED10 (CERES scores) showed that MED10 knockout significantly inhibited cell proliferation in the vast majority of GBM cell lines (Fig. 10h). These findings highlight the critical role of MED10 in GBM progression and its potential as a therapeutic target.

Knockdown MED10 inhibits the proliferation and migration of GBM cells

To validate the functional role of MED10, specific MED10-siRNAs were transfected into U87 and U118 cells, successfully knocking down MED10 expression (Fig. 11a). Subsequently, CCK-8 analysis demonstrated that MED10 knockdown significantly suppressed GBM cell proliferation (Fig. 11b,c). Results from the colony formation assay revealed that MED10 knockdown significantly reduced the colony-forming ability of GBM cells (Fig. 11d,e). Furthermore, the migration ability of GBM cells was notably suppressed after MED10 knockdown, as shown in the scratch assay (Fig. 11f,g). These results collectively suggest that MED10 plays a critical role in promoting GBM cell proliferation and migration, and its inhibition could offer a potential therapeutic strategy.

Discussion

GBM is a common, highly heterogeneous, and aggressive malignant primary brain tumor[1]. Standard therapeutic approaches, including surgery, chemotherapy, and radiotherapy, have made incremental progress; however, the prognosis for GBM remains exceptionally poor[7]. The molecular and clinical heterogeneity of GBM presents a major obstacle to effective treatment, as patients often exhibit varied responses to the same therapeutic regimen[9,10,34]. This highlights the urgent need for accurate patient stratification and the development of personalized treatment strategies tailored to the unique molecular characteristics of each tumor subtype.

A critical aspect of advancing GBM treatment lies in identifying therapeutic targets that are essential for tumor survival and progression. Historically, cancer therapeutic target discovery has focused on oncogenes and tumor suppressor genes with cancer-specific mutations, as these genes exhibit high specificity and are considered ideal candidates for targeted therapies. In recent years, the CRISPR/Cas9 system has revolutionized functional genomics by enabling precise and efficient genome editing[11,12]. Among its many applications, CRISPR-Cas9 screening has emerged as a transformative tool for genome-wide functional studies, facilitating the systematic
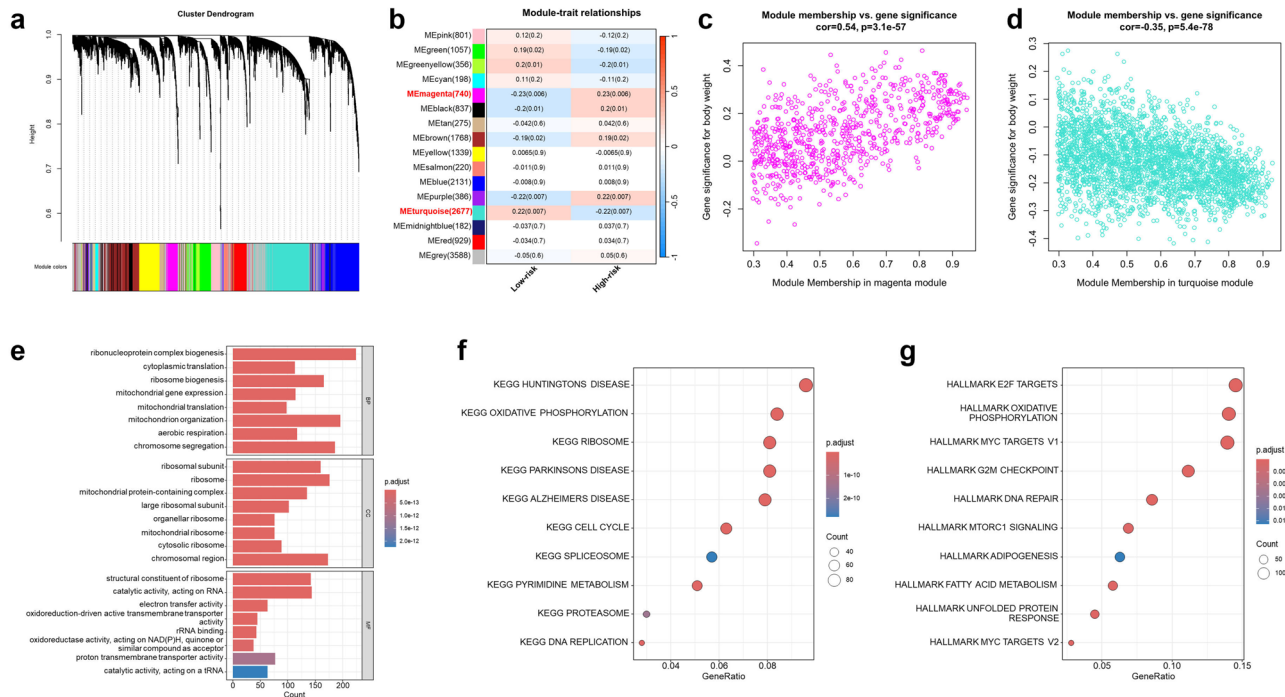
Fig. 7. WGCNA and functional enrichment analysis. (**a**) Cluster dendrogram of genes grouped into 16 modules using WGCNA. (**b**) Correlations between module eigengenes and glioblastoma risk groups. (**c,d**) Scatter plots demonstrating the relationship between module membership and gene significance for the magenta (**c**) and turquoise (**d**) modules, respectively. (**e**) GO enrichment analysis of genes in the significant modules. (**f**) KEGG pathway enrichment analysis of module genes. (**g**) Hallmark pathway enrichment analysis of module genes. *WGCNA* weighted correlation network analysis, *GO* gene ontology, *KEGG* kyoto encyclopedia of genes and genomes, *BP* biological process, *CC* cell component, *MF* molecular function.

identification of essential genes and pathways[17]. This technology has proven particularly powerful in uncovering therapeutic vulnerabilities in complex and treatment-resistant cancers such as GBM, offering new opportunities for the development of targeted therapies and precision oncology approaches[18–22].

Thus, this study aimed to identify potential targets for the prognostic assessment and precision treatment of GBM. Using CRISPR-Cas9 screening data from DepMap, we identified the proliferation-essential pathway and genes. We identified a set of 1618 genes that are essential for the proliferation of GBM cells and identified the E2F targets pathway as one of the most significantly enriched pathways driving GBM cell line proliferation. Based on univariate Cox regression, LASSO Cox regression, and multivariate Cox regression analyses, we established a prognostic signature consisting of CLSPN, HSP90B1, MED10, SAMM50, and TOMM20. This signature demonstrated the ability to stratify GBM patients into low-risk and high-risk groups with statistically significant differences in survival outcomes. Kaplan-Meier analysis revealed a significant difference between the two risk groups, with the high-risk group exhibiting markedly poorer outcomes compared to the low-risk group. The validity and reliability of this signature were further confirmed using both internal and external datasets.

Clinical association analysis showed that an elevated proliferation-related essential genes signature was significantly associated with unfavorable clinical features, such as advanced age and IDH WT status. In addition, we constructed a nomogram model by integrating the signature with other prognostic clinical factors, providing a visual statistical predictive tool for GBM patients' survival. The nomogram showed favorable performance in predicting 1-, 2-, and 3-year OS in GBM patients, as reflected by C-index and calibration plots. However, its clinical utility would benefit from further prospective validation.

To investigate the mechanisms underlying the prognostic differences between GBM patients in high- and low-risk groups, we analyzed biological process differences using WGCNA and GSEA. Both analyses revealed notable enrichment of proliferation-related pathways. Notably, the E2F targets pathway was consistently identified as the most significantly enriched pathway in both WGCNA and GSEA. This result aligns with our earlier discovery that the E2F targets pathway is one of the important drivers of GBM cell line proliferation. The E2F targets pathway plays a pivotal role in cell cycle regulation by controlling the transcription of genes essential for DNA replication, G1/S phase transition, and mitotic progression[35,36]. Dysregulation of the E2F pathway is a hallmark of many cancers, including GBM, where aberrant activation of E2F transcription factors drives uncontrolled proliferation and tumor progression[37–41].

The E2F pathway plays a complex and pivotal role in GBM progression and therapy resistance. Recent studies have shed light on its multifaceted functions, particularly in chromatin accessibility, tumorigenesis, and cell cycle regulation. E2F1, in cooperation with STAT3, activates the histone variant H2AZ, increasing chromatin accessibility and driving the transcription of cell cycle-related genes. This process promotes GBM stem cell
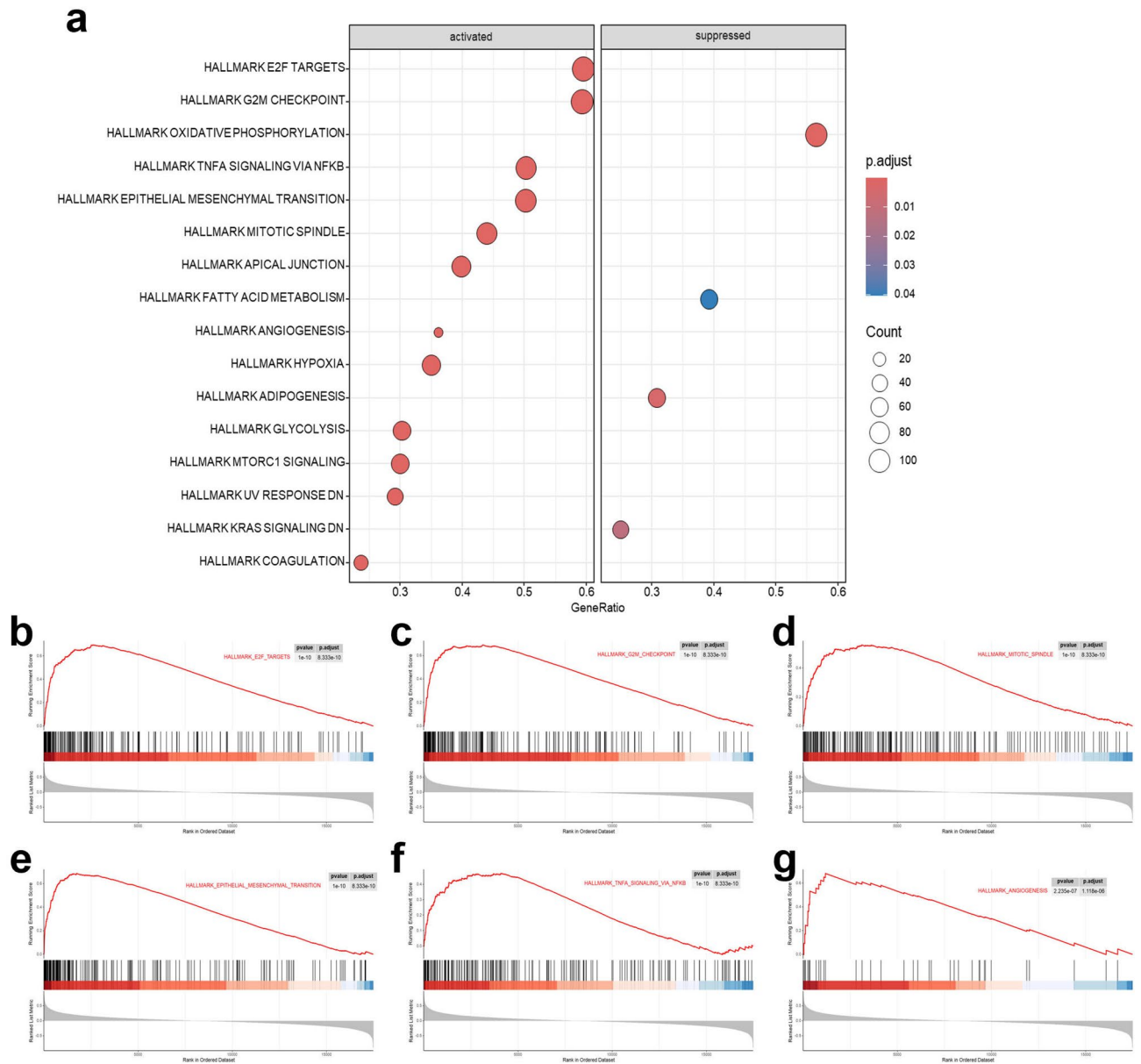
Fig. 8. GSEA of hallmark pathways associated with the proliferation-related essential genes signature in glioblastoma. (**a**) Bubble plot showing hallmark pathways significantly enriched in high-risk and low-risk glioblastoma groups. (**b**–**d**) Enrichment plots for hallmark pathways significantly activated in the high-risk group, including E2F targets (**b**), G2M checkpoint (**c**), and mitotic spindle (**d**), highlighting their roles in cell proliferation and tumor progression. (**e**–**g**) Enrichment plots for oncogenic pathways significantly activated in the high-risk group, including epithelial mesenchymal transition (**e**), TNF-α signaling via NF-κB (**f**), and angiogenesis (**g**), demonstrating their association with tumor invasion, inflammation, and vascularization. *GSEA* gene set enrichment analysis.

(GSC) proliferation and tumorigenicity. Notably, co-targeting E2F and STAT3 has shown significant potential in suppressing GSC-driven tumor growth in vivo[37]. Furthermore, E2F1 activity is modulated by NCAPG, a mitosis-related protein that enhances E2F1 transactivation via interaction with PARP1. This interaction establishes a positive feedback loop between NCAPG and E2F1, which further accelerates GBM progression, underscoring the therapeutic potential of targeting NCAPG[38]. E2F7, another member of the E2F family, promotes temozolomide resistance in GBM by regulating the G1/S cell cycle transition. The dysregulation of E2F7, driven by the lncRNA SNHG12, is strongly associated with poor patient survival and heightened chemotherapy resistance, further highlighting the E2F pathway's critical role in GBM malignancy and treatment failure[40]. Additionally, in GBM, alterations in upstream regulators of the E2F pathway, such as RB1 mutations, CDKN2A deletions, or CDK4/6 amplifications, frequently lead to hyperactivation of E2F targets[42–44]. This results in the persistent expression of genes involved in DNA synthesis, mitotic spindle assembly, and cell cycle checkpoints, promoting aggressive tumor growth and resistance to therapy. Collectively, these findings position the E2F pathway as a
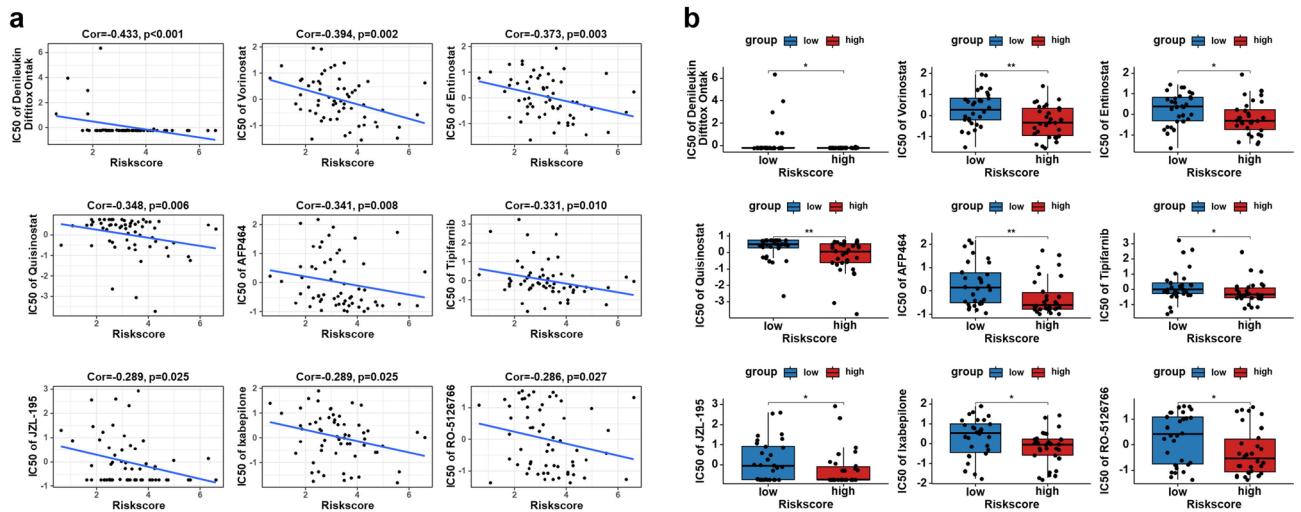
Fig. 9. Correlation between the proliferation-related essential genes signature and drug sensitivity. (**a**) Scatter plots showing the negative correlation between the risk score and IC50 values for several drugs, including Denileukin Diftitox Ontak, Vorinostat, Entinostat, Quisinostat, AFP464, Tipifarnib, JZL-195, Ixabepilone, and RO-5,126,766. (**b**) Boxplots comparing IC50 values for the above drugs between high-risk and low-risk groups. Statistical significance: $*p < 0.05$. *IC50* half maximal inhibitory concentration.

central regulator in GBM biology and a promising target for therapeutic intervention. Our findings reinforce the critical role of the E2F pathway in glioblastoma biology, as it was consistently identified as the most significantly enriched pathway across CRISPR-Cas9 screening and patient-derived transcriptomic data.

In our drug sensitivity analysis, several compounds including HDAC inhibitors (e.g., Vorinostat, Entinostat, Quisinostat) and the farnesyltransferase inhibitor Tipifarnib were identified as being more effective in high-risk GBM based on their negative correlation with the risk score. Although these compounds are not classical E2F inhibitors, increasing evidence supports their ability to modulate E2F signaling through indirect mechanisms. HDAC inhibitors are known to regulate E2F activity at multiple levels. They can suppress the transcription of E2F family members (e.g., E2F1, E2F3), disrupt the Rb-HDAC-E2F repressor complex to alter the expression of E2F target genes (e.g., Cyclin A, CDK1), and even modulate E2F-driven gene expression independently of the classical Rb/DREAM complex through acetylation-related mechanisms[45–47]. These effects may contribute to their preferential efficacy in tumors with E2F pathway activation, such as high-risk GBM. Tipifarnib, while primarily a farnesyltransferase inhibitor targeting HRAS, has also been linked to E2F pathway regulation. It can suppress upstream RAS/MAPK and PI3K/AKT signaling, thereby reducing Rb phosphorylation and limiting E2F activation[48]. Notably, high E2F target gene expression has been reported as a predictive biomarker for Tipifarnib sensitivity in hepatocellular carcinoma[49]. In addition, combination strategies using Tipifarnib and PI3K inhibitors have shown enhanced anti-tumor efficacy in HRAS-mutant head and neck cancers, potentially through modulation of E2F-driven cell cycle progression[50]. These findings provide a plausible mechanistic explanation for the association between the identified compounds and the high-risk GBM subtype characterized by E2F pathway activation. They also highlight the potential of these agents as therapeutic candidates for further investigation in E2F-driven glioblastoma.

MED10, identified through random forest analysis, emerged as the most critical gene among the five proliferation-related essential genes in our prognostic signature. MED10 encodes a component of the Mediator complex, a multiprotein complex that bridges transcription factors and RNA polymerase II, playing a crucial role in regulating gene expression[51]. Dysregulation of Mediator complex components has been implicated in various cancers, where they contribute to aberrant transcriptional activation of oncogenic pathways[52–54]. In GBM, our findings suggest that MED10 is not only essential for tumor cell proliferation but is also associated with poor patient outcomes, as supported by Kaplan-Meier survival analysis. The significant correlation between high MED10 expression and shorter OS highlights its potential as both a prognostic biomarker and a therapeutic target.

Further functional experiments demonstrated that MED10 knockdown significantly inhibited GBM cell proliferation and migration, underscoring its role in driving tumor progression. Given its central role within the Mediator complex, MED10 may regulate key oncogenic pathways, including the E2F targets pathway, which was identified as a critical driver of GBM proliferation in our study. Future research should explore how MED10 interacts with the E2F pathway and other proliferation-related pathways, as well as investigate the potential of targeting MED10 directly or indirectly to disrupt GBM growth and improve therapeutic outcomes. Collectively, these findings position MED10 as a promising candidate for further investigation in GBM biology and therapy.

Compared to previous GBM prognostic models that primarily rely on transcriptomic or immune-related features, our study introduces a functionally grounded approach by leveraging CRISPR-Cas9 screening data to identify GBM-specific proliferation-related essential genes. For example, studies by Chen et al. and Liu et al. constructed gene signatures based on differentially expressed genes or immune checkpoints but lacked functional
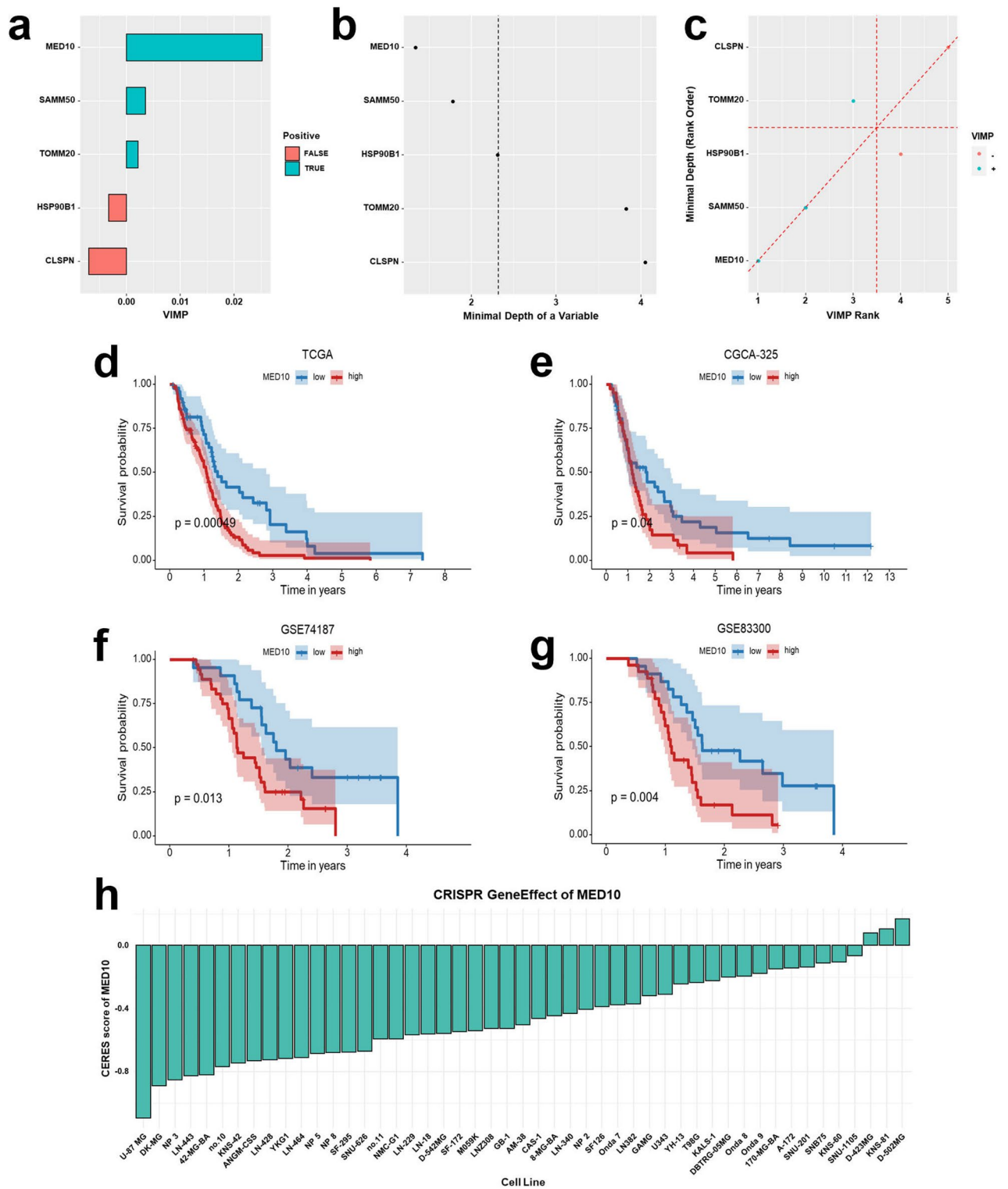
Fig. 10. Identification of MED10 as the most significant proliferation-related essential gene in glioblastoma. (**a**–**c**) Random forest analysis identifying MED10 as the most important gene among the five proliferation-related essential genes. (**d**–**g**) Kaplan-Meier survival curves across multiple datasets (TCGA, CGGA-325, GSE74187, GSE83300) showing significantly worse overall survival in glioblastoma patients with high MED10 expression compared to those with low expression. (**h**) CERES scores of MED10 in 49 glioblastoma cell lines. *TCGA* the cancer genome atlas, *CGGA* Chinese glioma genome atlas, *VIMP* variable importance.
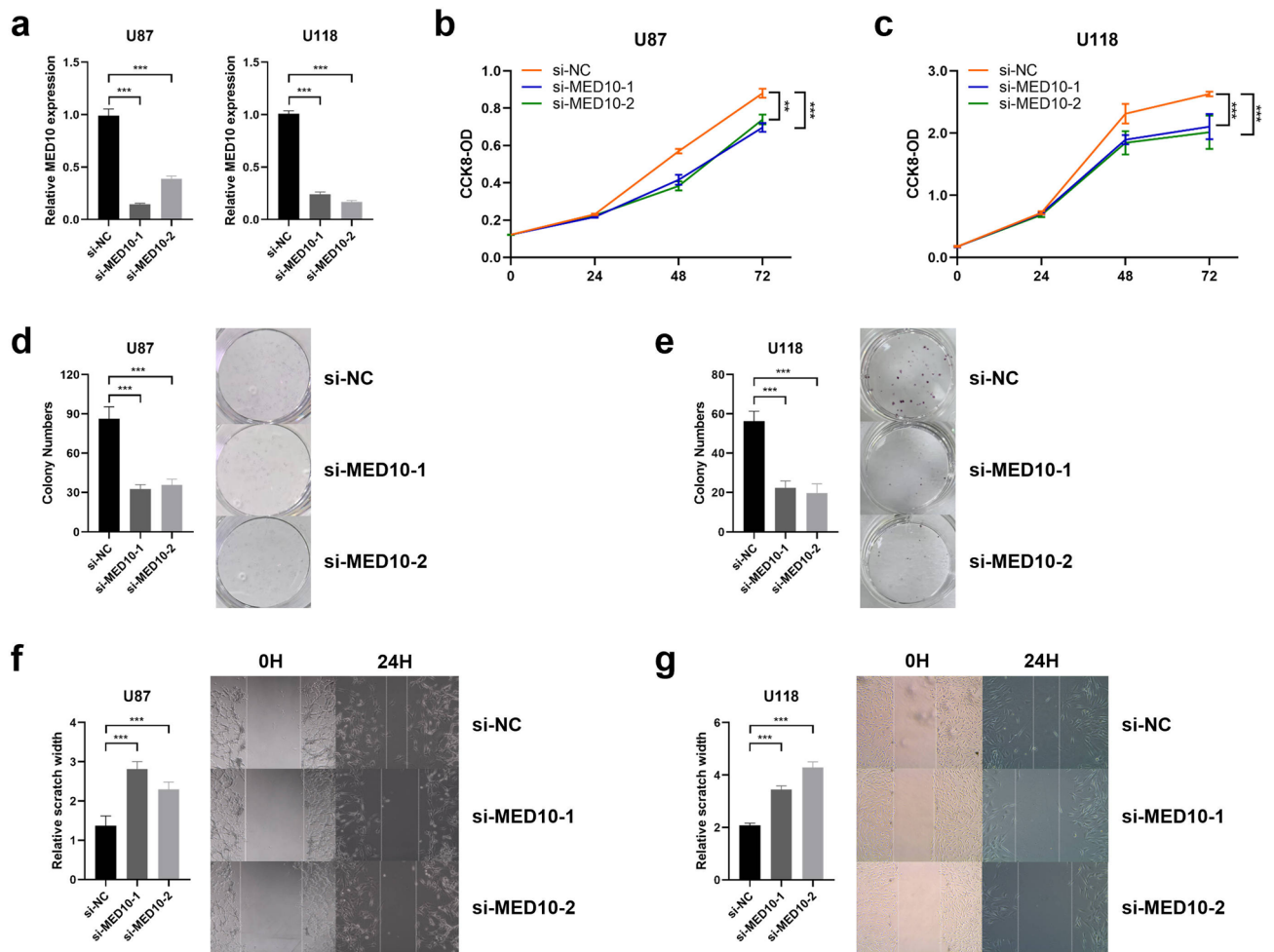
Fig. 11. Knockdown of MED10 inhibits glioblastoma cell proliferation, colony formation, and migration. (**a**) Identification of MED10 knockdown. (**b,c**) CCK-8 assay demonstrating the inhibition of cell proliferation in U87 (**b**) and U118 (**c**) cells following MED10 knockdown. (**d,e**) Colony formation assays showing a significant reduction in the number of colonies in U87 (**d**) and U118 (**e**) cells after MED10 knockdown. (**f,g**) Wound healing assays illustrating the suppression of migration in U87 (**f**) and U118 (**g**) cells following MED10 knockdown.

validation or mechanistic exploration[24,25]. In contrast, our model identifies genes that have been experimentally validated as essential for GBM cell survival, enhancing both prognostic accuracy and biological interpretability. Moreover, through GSEA and WGCNA analyses, we uncover E2F pathway activation as a central mechanism in high-risk GBM, and demonstrate that one of the signature genes, MED10, promotes GBM cell proliferation and migration, thus bridging prognostic modeling with potential therapeutic targets.

This study has several limitations that should be acknowledged. First, it is retrospective in nature, which may introduce inherent biases. Second, although external validation cohorts were used, additional independent studies—particularly prospective clinical cohorts—are needed to confirm the prognostic value and clinical applicability of the proliferation-essential gene signature. Third, while MED10 was functionally validated in vitro, the mechanistic role of this gene in GBM progression requires further investigation. Additionally, drug sensitivity analysis was based on the NCI-60 cell line panel, which includes only a limited number of GBM-derived cell lines. To address this limitation, we performed a pan-cancer analysis to identify compounds potentially associated with the risk score. Although informative, this exploratory approach warrants further validation in glioblastoma-specific models. Finally, due to the retrospective nature of the datasets, detailed treatment and clinical management information were not uniformly available, which may introduce unmeasured confounding factors affecting survival outcomes and gene expression. Despite these limitations, our study provides a functionally informed prognostic model and identifies MED10 as a candidate therapeutic target. The integration of CRISPR-based essentiality screening, transcriptomic data, and experimental validation offers a multi-dimensional perspective on GBM biology. Future studies should focus on mechanistic dissection and clinical validation to further explore the translational potential of these findings.

Conclusions

In this study, we identified proliferation-related essential genes in GBM using genome-wide CRISPR-Cas9 screening data and highlighted the E2F targets pathway as a potential key driver of tumor proliferation. Based on these findings, we developed and validated a five-gene prognostic signature (CLSPN, HSP90B1, MED10, SAMM50, TOMM20) that stratified patients into distinct survival risk groups across multiple independent cohorts. Among these genes, MED10 emerged as a potential key contributor, supported by random forest analysis and preliminary functional experiments indicating its involvement in GBM cell proliferation and migration. While these findings offer novel insights into GBM biology, we acknowledge that further mechanistic investigations and prospective clinical validation are needed to fully elucidate the roles of MED10 and the E2F pathway. Nevertheless, our results provide a foundation for future studies exploring personalized therapeutic strategies and functionally informed biomarkers aimed at improving outcomes for GBM patients.

Data availability

Data availability statementThe datasets analyzed in the current study are available from TCGA (https://portal.gdc.cancer.gov/), GEO (https://www.ncbi.nlm.nih.gov/geo/), CGCA (https://www.cgga.org.cn/) and Depmap (https://depmap.org/).

References

1. Sipos, D. et al. Glioblastoma: clinical presentation, multidisciplinary management, and Long-Term outcomes. *Cancers (Basel)*. **17**, 146 (2025).
2. Poursaeed, R., Mohammadzadeh, M. & Safaei, A. A. Survival prediction of glioblastoma patients using machine learning and deep learning: a systematic review. *BMC Cancer*. **24**, 1581 (2024).
3. Pinto-Fraga, J. et al. Protein kinase inhibitors as targeted therapy for glioblastoma: a meta-analysis of randomized controlled clinical trials. *Pharmacol. Res.* **212**, 107528 (2025).
4. Valerius, A. R. et al. Review of novel surgical, radiation, and systemic therapies and clinical trials in glioblastoma. *Int. J. Mol. Sci.* **25**, 10570 (2024).
5. Wang, L. et al. Recent advances in nanoenzymes based therapies for glioblastoma: overcoming barriers and enhancing targeted treatment. *Adv. Sci. (Weinh)*. **12**, e2413367 (2025).
6. Xiong, Y. et al. Nanoparticle-based drug delivery systems to modulate tumor immune response for glioblastoma treatment. *Acta Biomater.* **194**, 38–57 (2025).
7. Khiabani, N. A. et al. Glioblastoma therapy: state of the field and future prospects. *Life Sci.* **359**, 123227 (2024).
8. Kricha, A. et al. Glioblastoma-associated macrophages: A key target in overcoming glioblastoma therapeutic resistance. *Cytokine Growth Factor. Rev.* **80**, 97–108 (2024).
9. Tang, Q. et al. Novel strategies to overcome chemoresistance in human glioblastoma. *Biochem. Pharmacol.* **230**, 116588 (2024).
10. Tataranu, L. G. et al. Glioblastoma tumor microenvironment: an important modulator for tumoral progression and therapy resistance. *Curr. Issues Mol. Biol.* **46**, 9881–9894 (2024).
11. Garg, P. et al. Unveiling the potential of gene editing techniques in revolutionizing Cancer treatment: A comprehensive overview. *Biochim. Biophys. Acta Rev. Cancer*. **1880**, 189233 (2025).
12. Di Carlo, E. & Sorrentino, C. State of the Art CRISPR-based strategies for cancer diagnostics and treatment. *Biomark. Res.* **12**, 156 (2024).
13. Xu, W., Zhang, S., Qin, H. & Yao, K. From bench to bedside: cutting-edge applications of base editing and prime editing in precision medicine. *J. Transl Med.* **22**, 1133 (2024).
14. Lei, T. et al. Leveraging CRISPR gene editing technology to optimize the efficacy, safety and accessibility of CAR T-cell therapy. *Leukemia* **38**, 2517–2543 (2024).
15. Madorsky Rowdo, F. P. et al. Kinome-Focused CRISPR-Cas9 screens in African ancestry Patient-Derived breast Cancer organoids identify essential kinases and synergy of EGFR and FGFR1 Inhibition. *Cancer Res.* **85**, 551–566 (2025).
16. Li, X. G. et al. Genome-wide CRISPR-Cas9 screening identifies ITGA8 responsible for abivertinib sensitivity in lung adenocarcinoma. *Acta Pharmacol. Sin.* **46**, 1419–1432 (2025).
17. Tsherniak, A. et al. Defining a Cancer dependency map. *Cell* **170**, 564–576e16 (2017).
18. Wang, Y. X. et al. CRISPR-Cas9 screening identified novel subtypes of cutaneous melanoma based on essential cancer genes. *Arch. Dermatol. Res.* **317**, 86 (2024).
19. Li, S. & Han, T. Frequent loss of FAM126A expression in colorectal cancer results in selective FAM126B dependency. *iScience* **27**, 109646 (2024).
20. Yu, L. et al. Prognostic and chemotherapeutic response prediction by proliferation essential gene signature: investigating POLE2 in bladder cancer progression and cisplatin resistance. *J. Cancer*. **15**, 1734–1749 (2024).
21. Liu, C. et al. Novel molecular classification and prognosis of papillary renal cell carcinoma based on a large-scale CRISPR-Cas9 screening and machine learning. *Heliyon* **10**, e23184 (2024).
22. Zhang, H. et al. Screening and identification of CNIH4 gene associated with cell proliferation in gastric cancer based on a large-scale CRISPR-Cas9 screening database DepMap. *Gene* **850**, 146961 (2023).
23. Cao, M., Zhang, W., Chen, J. & Zhang, Y. Identification of a coagulation-related gene signature for predicting prognosis in recurrent glioma. *Discov Oncol.* **15**, 642 (2024).
24. Chen, C. et al. Developing and validating a prognostic disulfidptosis-related signature for glioblastoma: predicting radioresistance and synergestic effect with immunotherapy. *J. Cancer Res. Clin. Oncol.* **151**, 112 (2025).
25. Liu, X. & Liu, X. A novel immune-related gene prognostic signature combining immune cell infiltration and immune checkpoint for glioblastoma patients. *Transl Cancer Res.* **13**, 6136–6153 (2024).
26. Xu, S. et al. Using clusterprofiler to characterize multiomics data. *Nat. Protoc.* **19**, 3292–3320 (2024).
27. Kanehisa, M. & Goto, S. KEGG: Kyoto encyclopedia of genes and genomes. *Nucleic Acids Res.* **28**, 27–30 (2000).
28. Kanehisa, M. Toward Understanding the origin and evolution of cellular organisms. *Protein Sci.* **28**, 1947–1951 (2019).
29. Kanehisa, M., Furumichi, M., Sato, Y. & Kawashima, M. Ishiguro-Watanabe, M. KEGG for taxonomy-based analysis of pathways and genomes. *Nucleic Acids Res.* **51**, D587–D592 (2023).
30. Friedman, J., Hastie, T. & Tibshirani, R. Regularization paths for generalized linear models via coordinate descent. *J. Stat. Softw.* **33**, 1–22 (2010).
31. Robin, X. et al. pROC: an open-source package for R and S + to analyze and compare ROC curves. *BMC Bioinform.* **12**, 77 (2011).

32. Blanche, P., Dartigues, J. F. & Jacqmin-Gadda, H. Estimating and comparing time-dependent areas under receiver operating characteristic curves for censored event times with competing risks. *Stat. Med.* **32**, 5381–5397 (2013).
33. Langfelder, P. & Horvath, S. WGCNA: an R package for weighted correlation network analysis. *BMC Bioinform.* **9**, 559 (2008).
34. White, J., White, M. P. J., Wickremesekera, A., Peng, L. & Gray, C. The tumour microenvironment, treatment resistance and recurrence in glioblastoma. *J. Transl Med.* **22**, 540 (2024).
35. Engeland, K. Cell cycle regulation: p53-p21-RB signaling. *Cell. Death Differ.* **29**, 946–960 (2022).
36. Kassab, A., Gupta, I. & Moustafa, A. E. A. Role of E2F transcription factor in oral cancer: recent insight and advancements. *Semin Cancer Biol.* **92**, 28–41 (2023).
37. Yoon, J. et al. E2F and STAT3 provide transcriptional synergy for histone variant H2AZ activation to sustain glioblastoma chromatin accessibility and tumorigenicity. *Cell. Death Differ.* **29**, 1379–1394 (2022).
38. Hou, J. et al. Nonstructural maintenance of chromatin condensin I complex subunit G promotes the progression of glioblastoma by facilitating Poly (ADP-ribose) polymerase 1-mediated E2F1 transactivation. *Neuro Oncol.* **25**, 2015–2027 (2023).
39. Yu, H., Zhang, D., Li, Z. & Wang, M. E2F transcription factor 8 promotes proliferation and radioresistance in glioblastoma. *Pathol. Res. Pract.* **216**, 153030 (2020).
40. Lu, C. et al. DNA-methylation-mediated activating of LncRNA SNHG12 promotes Temozolomide resistance in glioblastoma. *Mol. Cancer.* **19**, 28 (2020).
41. Luo, C. et al. SRSF9 promotes cell proliferation and migration of glioblastoma through enhancing CDK1 expression. *J. Cancer Res. Clin. Oncol.* **150**, 292 (2024).
42. Barresi, V. et al. IDH-wild type glioblastomas featuring at least 30% giant cells are characterized by frequent RB1 and NF1 alterations and hypermutation. *Acta Neuropathol. Commun.* **9**, 200 (2021).
43. Minami, J. K. et al. CDKN2A deletion remodels lipid metabolism to prime glioblastoma for ferroptosis. *Cancer Cell.* **41**, 1048–1060e9 (2023).
44. Cen, L. et al. p16-Cdk4-Rb axis controls sensitivity to a cyclin-dependent kinase inhibitor PD0332991 in glioblastoma xenograft cells. *Neuro Oncol.* **14**, 870–881 (2012).
45. Han, R., Yang, H., Li, Y., Ling, C. & Lu, L. Valeric acid acts as a novel HDAC3 inhibitor against prostate cancer. *Med. Oncol.* **39**, 213 (2022).
46. Villamar-Cruz, O. et al. A PTP1B-Cdk3 signaling Axis promotes cell cycle progression of human glioblastoma cells through an Rb-E2F dependent pathway. *Mol. Cell. Biol.* **43**, 631–649 (2023).
47. Barrett, A. K. et al. HDAC activity is dispensable for repression of cell-cycle genes by DREAM and E2F:RB complexes. *Nat. Commun.* **15**, 4450 (2024).
48. Scerri, J. et al. PKC-mediated phosphorylation and activation of the MEK/ERK pathway as a mechanism of acquired trastuzumab resistance in HER2-positive breast cancer. *Front. Endocrinol. (Lausanne).* **13**, 1010092 (2022).
49. Zhang, B., Chang, B., Wang, L. & Xu, Y. Three E2F target-related genes signature for predicting prognosis, immune features, and drug sensitivity in hepatocellular carcinoma. *Front. Mol. Biosci.* **10**, 1266515 (2023).
50. Manikandan, D. B. et al. Anti-PD1 prolongs the response of PI3K and Farnesyl transferase Inhibition in HRAS- and PIK3CA-mutant head and neck cancers. *Neoplasia* **63**, 101157 (2025).
51. Soutourina, J. Transcription regulation by the mediator complex. *Nat. Rev. Mol. Cell. Biol.* **19**, 262–274 (2018).
52. Wu, C. C. et al. MED10 drives the oncogenicity and refractory phenotype of bladder urothelial carcinoma through the upregulation of hsa-miR-590. *Front. Oncol.* **11**, 744937 (2021).
53. Han, X., Liu, H., Tang, X. & Zhao, Y. Knockdown of mediator complex subunit 27 suppresses gastric cancer cell metastasis and angiogenesis via Wnt/β-catenin pathway. *Tissue Cell.* **79**, 101973 (2022).
54. Sooraj, D. et al. MED12 and BRD4 cooperate to sustain cancer growth upon loss of mediator kinase. *Mol. Cell.* **82**, 123–139e7 (2022).

Acknowledgements

Author contributions

Author contributionsJYH and WTX designed the research. XR, WTX, XRY, and KC collected and analyzed the data. KC drafted the manuscript. WTX and XRY prepared the figures. JYH revised the manuscript. All the authors have read and approved the final version of the manuscript.

Funding

Declarations

Competing interests

The authors declare no competing interests.

Additional information

Supplementary Information The online version contains supplementary material available at https://doi.org/10.1038/s41598-025-07815-8.

Correspondence and requests for materials should be addressed to W.-t.X. or J.-y.H.

Reprints and permissions information is available at www.nature.com/reprints.

Publisher's note Springer Nature remains neutral with regard to jurisdictional claims in published maps and institutional affiliations.